Brownian dynamics simulation of electrooptical transients for solutions of rigid macromolecules

Jan Antosiewicz, Tomasz Grycuk, and Dietmar Porschke

Citation: The Journal of Chemical Physics **95**, 1354 (1991); doi: 10.1063/1.461785
View online: http://dx.doi.org/10.1063/1.461785
View Table of Contents: http://scitation.aip.org/content/aip/journal/jcp/95/2?ver=pdfcov
Published by the AIP Publishing

Brownian dynamics simulation of electrooptical transients for solutions of rigid macromolecules

Jan Antosiewicz and Tomasz Grycuk
Department of Biophysics, Warsaw University, 02-089 Warsaw, Poland

Dietmar Porschke
Max Planck Institut für Biophysikalische Chemie, 3400 Göttingen-Nikolausberg, Germany

(Received 19 February 1991; accepted 10 April 1991)

The overall rotational diffusion of rigid macromolecules in solution under rectangular electric field pulses is simulated by Brownian dynamics. We describe computer programs for the simulation of electrooptical transients without restrictions on molecular parameters or electric field strengths. The programs are used first for the calculation of electrooptical transients of molecules with cylindrical symmetry with induced or permanent dipole moments. The simulated data are consistent with analytical results, valid, e.g., for the limit of zero field strength, but have been extended to ranges, where analytical results are not available. Among the two time constants required for fitting of rise curves for permanent dipoles, the smaller one proves to be almost independent of the electric field strength E, whereas the larger one decreases strongly with increasing E; at high E values the two time constants are very close to each other. By comparison of simulated and experimental transients it is possible to analyze hidden contributions, e.g., of an induced dipole moment in the presence of a dominant permanent moment. The simulations are extended to the case of a molecule without symmetry, tRNA, which is used to characterize the hydrodynamic coupling of translational and rotational motion. We show that in this case the influence of hydrodynamic coupling on the dipole moment, the limiting reduced dichroism and the risetime constants derived from electrooptical experiments is very small ($\leqslant 10\%$).

I. INTRODUCTION

Measurements of electrooptical transients for solutions of anisotropic polymers, particularly biological macromolecules, have been used for a long time as tools for the analysis of the molecular long-range structure, internal dynamics and electric moments.[1-5] Interpretation of the experimental results requires a general theory for the calculation of transient electrooptical signals from diffusion coefficients for overall and internal motions of the polymers as well as from electric and optical parameters. There are many examples of investigations devoted to theoretical modeling of transient electrooptical signals.[6-17] Usually the available procedures can be applied only within certain limits, for example, the limit of very low or very high electric field strengths. Such limitations may be avoided by simulations of electrooptical transients using the method of Brownian dynamics.[18,19] This method has been applied with great success for the simulation of the decay of fluorescence anisotropies,[20-22] but has not been used yet for the analysis of electrooptical transients.

In our present contribution we describe a Brownian dynamics algorithm for the simulation of overall rotational diffusion of rigid particles under the influence of rectangular electric field pulses. The algorithm is applied for the simulation of electrooptical transients for solutions of rigid particles. As models we have selected two particles of different size with cylindrical symmetry: the two models are characterized by the rotational diffusion coefficient corresponding to that of a DNA with 84 base pairs and of α-chymotrypsin, respectively. For these models we analyze the dependence of electrooptical rise curves on the electric field strength. In addition we have simulated electrooptical transients of $tRNA^{Phe}$ (yeast) as an example of a nonsymmetric molecule. For this special case we have characterized the influence of translational–rotational coupling[23] on electrooptical rise curves and on the permanent dipole moment derived from the stationary reduced dichroism at different field strengths.

II. DESCRIPTION OF THE PROGRAM

A. General Idea

The program calculates electrooptical transients[2] for a "solution" containing N independent identical particles, which are exposed to a rectangular electric field pulse of strength E. Initially the particles are distributed uniformly among $8\pi^2$ orientational states. This is achieved by sampling three Eulerian angles for each particle:[24] ϕ and ψ from a uniform distribution over the range $[0; 2\pi]$, θ over the range $[0; \pi]$ with a probability proportional to $\sin\theta/2$.[25] Then, an electric field E is applied for a time interval t_{pulse} and the trajectories of rotational movements of each particle are calculated during some time t_{obs}.

We define two different coordinate systems: the particle coordinate system (PCS) is given by the system of principal axes of the particle rotational diffusion tensor. In this coordinate system the generalized diffusion tensor[23] D, the extinction coefficients tensor A, the polarizability tensor P, and the dipole moment vector μ, characterizing the particle, are as-

 0021-9606/91/141354-07$03.00

sumed to be known. The orientation of each particle in the "laboratory coordinate system" (LCS) is defined by the rotation matrix O, which transforms the PCS to the LCS. Our convention for the sampled Eulerian angles is given by the following procedure: if O is the rotation matrix written according to equation (4-46) in Goldstein's book[24] and if A is the extinction tensor written in PCS, then $O^T AO$ gives the components of this tensor in LCS (O^T is the transposed O).

When the incident light is polarized parallel to the z axis, is directed towards the x axis of LCS and the electric field vector is directed parallel to the z axis, the contribution of each particle to the reduced linear dichroism of the solution is given by

$$\Delta\epsilon/\bar{\epsilon} = \frac{A_{zz,\mathrm{LCS}} - A_{yy,\mathrm{LCS}}}{\bar{A}}, \tag{1}$$

where A_{ii} are the components of the absorbance tensor in the direction of the i axis and $\bar{A}$ is the mean extinction coefficient of the solution. The reduced linear dichroism of the solution is calculated as the average of all individual contributions. The resulting data are evaluated exactly as standard experimental data: dichroism rise and decay time constants were determined by an efficient routine[26] for exponential fitting; stationary values of the reduced linear dichroism as function of the electric field strength were used for the determination of the nature and the magnitudes of electric moments.[27]

B. Rotation vector formalism

The rotational movement of a particle may be described by rotation matrices O_i for each individual rotational step, which result in an overall rotation matrix $O_I = O_i O_{i-1} \ldots O_2 O_1$ describing the orientation of the particle with respect to the reference coordinate system after i rotational steps. However, this procedure may lead to an accumulation of errors: because of the limited computer accuracy the rotation matrix O_I may not be orthogonal anymore after some number of multiplications. Thus, in our present investigation we use the formalism of rotation vectors[28] to describe the rotational motion of particles. Application of this formalism is equivalent to orthogonalization of the O_I matrices after each step of simulation. The direction of the rotation vector $\mathbf{k}$ indicates the orientation of the rotation axis and its length corresponds to the tangens of half of the overall rotation angle χ. Rotation vectors add according to the following rule: two subsequent rotations performed in the same coordinate system, described by rotation vectors $\mathbf{k}_1$ and $\mathbf{k}_2$, lead to the resulting rotation vector[28]

$$\mathbf{k}_3 = (1 - \mathbf{k}_1 \cdot \mathbf{k}_2)^{-1}(\mathbf{k}_1 + \mathbf{k}_2 + \mathbf{k}_1 \times \mathbf{k}_2), \tag{2}$$

where "$\cdot$" and "$\times$" indicate the scalar and the vector product of vectors, respectively.

For calculation of the components of the particle extinction tensor in LCS, the rotation vector $\mathbf{k}$ is transformed to the rotation matrix O. The elements of this matrix may be easily obtained by the following transformation,[28] which is valid for arbitrary vectors $\mathbf{r}$:

$$\mathbf{r}_{\mathrm{PCS}} = \mathbf{r}_{\mathrm{LCS}} \cos\chi - \mathbf{u} \times \mathbf{r}_{\mathrm{LCS}} \sin\chi + (1 - \cos\chi)\mathbf{u}(\mathbf{u} \cdot \mathbf{r}_{\mathrm{LCS}}), \tag{3}$$

where $\mathbf{u} = \mathbf{k}/k$. Comparison with the result of explicitly written $\mathbf{r}_{\mathrm{PCS}} = O\mathbf{r}_{\mathrm{LCS}}$ provides the equations for the components of the matrix O.

Eulerian angles, initially sampled for random distribution of each particle (cf. above), may be easily converted into components of rotation vectors by the following set of equations:[28]

$$k_1 = \frac{\sin\theta(\cos\phi + \cos\psi)}{(1 + \cos\theta)[1 + \cos(\phi + \psi)]},$$
$$k_2 = \frac{\sin\theta(\sin\psi - \sin\phi)}{(1 + \cos\theta)[1 + \cos(\phi + \psi)]}, \tag{4}$$
$$k_3 = \frac{\sin(\phi + \psi)}{1 + \cos(\phi + \psi)}.$$

C. The algorithm

The simulation of the rotational diffusion of the macromolecules in solution is based on the Brownian dynamics algorithm described by Ermak and McCammon.[18] First we rewrite their Eq. (15) for *translational* movement of one rigid particle:

$$\mathbf{r} = \mathbf{r}^0 + \frac{D_t \mathbf{F}^0}{kT}\Delta t + \mathbf{R}_{\mathrm{rnd}}(\Delta t), \tag{5}$$

where variables marked with the superscript "0" are to be evaluated at the start of the time step, $\mathbf{r}$ indicates the position of the particle, D_t is the translational diffusion tensor, $\mathbf{F}$ is the external force vector, and $\mathbf{R}_{\mathrm{rnd}}$ is the "random step vector." The mean value of the random step vector is zero and its variance–covariance matrix is given by

$$\langle R_i R_j \rangle = 2D_{t,ij}\Delta t, \tag{6}$$

where $i,j = x,y,z$. Equation (5) is valid for time steps Δt much longer than the momentum relaxation time $m\bar{D}_t/kT$, where m is the mass of the particle and $\bar{D}_t$ is the mean translational diffusion coefficient. Equation (5) is written in LCS, but equally well we may refer all equations to PCS; then LCS is moved at each step. Because this is more convenient for programming of rotational movement, all following equations are written in PCS; i.e., all vectors and tensors, if not stated otherwise, are given in PCS.

In analogy to the above equation, we define the corresponding equation for rotational movement of whole particles using the rotation vector formalism. Let us denote by $\mathbf{k}^0$ the rotation vector,[28] which decribes the orientation of the LCS with respect to the PCS at "zero" time; then the orientation after time step Δt is given by

$$\mathbf{k} = \mathbf{k}^0 \oplus \frac{D_r \mathbf{T}^0 \Delta t}{kT} + \mathbf{K}_{rnd}(\Delta t), \tag{7}$$

where the superscript 0 denotes again the appropriate value at the start of time step Δt, D_r is the rotational diffusion tensor, $\mathbf{T}^0$ the torque exerted on the particle, and $\mathbf{K}_{rnd}(\Delta t)$ a random rotational step. The three independent components of random rotational steps, contributing to $\mathbf{K}_{rnd}(\Delta t)$, are sampled from one-dimensional Gaussian distributions with zero mean value and a standard deviation corresponding to $(2D_{r,ii}\Delta t)^{1/2}$ where $i = x,y,z$. The two last terms of Eq. (7) add like normal vectors because they refer to the same mo-

ment of time. The vector obtained by addition has the direction of the rotation axis and the length of the rotation angle. This vector is converted to the rotation vector just by assignment of the correct length (tangens of half the rotation angle, cf. above). The resulting rotation vector is added to the rotation vector describing the previous orientation according to Eq. (2). The procedure for the calculation of the rotation vector from the last two terms of Eq. (7) and its addition to the previous rotation vector is indicated by the special symbol $\oplus$.

For a more realistic description of the rotational motion in an electric field we have to add another important factor to Eq. (7). Usually biological macromolecules are polyelectrolytes with considerable net charges and thus show electrophoretic movement; this translational motion may cause a rotational one. The coupling between translational and rotational motions of the particle[23] is accounted for in Eq. (7) by addition of a new term, which describes the rotational velocity forced by the translational one

$$\mathbf{k} = \mathbf{k}^0 \oplus \frac{D_r \mathbf{T}_P^0 \Delta t}{kT} + \frac{q D_{c,P} \mathbf{E}^0 \Delta t}{kT} + \mathbf{K}_{rnd}(\Delta t). \tag{8}$$

$D_{c,P}$ is the translation–rotation coupling tensor, which depends on the choice of origin P of PCS within the molecule, $\mathbf{E}^0$ is the electric field vector in PCS, and q is the charge of the particle. Now the components of random rotational steps $\mathbf{K}_{rnd}(\Delta t)$ are not independent anymore because of the coupling between translational and rotational motions. We have to use a generalized random step, which includes three translational and three rotational components. The mean values of the six components are zero, but their variance–covariance matrix is determined by the whole generalized diffusion tensor, which is given in direct analogy to Eq. (6). For the purpose of our present investigation we are interested only in the components of rotational random steps, which are obtained as follows: first six random numbers from a normal distribution with zero mean and standard deviation 1.0 are sampled and scaled to standard deviation $(2\times\Delta t)^{1/2}$; subsequently these six random numbers are used to calculate three rotational steps according to the Eqs. (16) and (17) from the paper by Ermak and McCammon.[18]

The addition rules for the components of Eq. (8) are the same as in the case of Eq. (7). As was indicated in Eq. (8), the tensor $D_{c,P}$ depends on the location of the coordinate system within the particle, but the expression

$$\frac{D_r \mathbf{T}_P^0 \Delta t}{kT} + \frac{q D_{c,P} \mathbf{E}^0 \Delta t}{kT}$$

does not depend on that choice.[14] Thus, the choice of the point P within the particle is not very important. Nevertheless we always have P at the so-called "center of diffusion"[23] and thus our tensor $D_{c,P}$ is symmetric.

During simulation each particle is rotated under the influence of the stochastic torque, the electric force torque, and, if the particle is charged, the hydrodynamic torque, resulting from translational–rotational coupling. Obviously, the last two torques are active only in the presence of an *external* electric field. The components of the electric field vector $\mathbf{E}$ in PCS, required for calculation of electrical and hydrodynamic torques, are obtained from the equation

$$\mathbf{E}_{PCS} = O\,\mathbf{E}_{LCS}. \tag{9}$$

The components of $\mathbf{E}_{LCS}$ are simply $(0;0;E)$. The calculated components of the electric field in PCS are used to calculate the resulting dipole moment from the polarizability tensor and finally the torque due to the electric force according to the standard equation.

The time steps applied during simulation must satisfy the condition $\Delta t \gg I_{ii} D_{r,ii}/kT$, where I is the tensor of the moments of inertia.

D. The algorithm for particles with cylindrical symmetry

For macromolecules with cylindrical symmetry the program can be simplified considerably with respect to that required for the general case. For particles with cylindrical symmetry we have to know only the angle of the main axis of each particle with respect to the z axis of LCS. As input data we need the scalar rotational diffusion coefficient for the reorientation of the long molecular axis D, the limiting reduced dichroism of the particles at infinite electric field $(\Delta\epsilon/\bar{\epsilon})_\infty$, the dipole moment μ and/or the polarizability p along the main axis. During simulation the temporal changes of $\cos\theta$ are recorded, where θ is the angle between the main axis of the particle and the z axis of LCS. First N values of $\cos\theta$ are sampled for an initially uniform random distribution. For that purpose we take N random numbers r_{rnd} from a uniform [0,1] distribution and use equation

$$\cos\theta = 2\cdot r_{rnd}^{-1}. \tag{10}$$

Subsequently individual $\cos\theta$ values are varied by sampling two random numbers r_{g1} and r_{g2} from a normal Gaussian distribution with zero mean and a standard deviation $(2D\Delta t)^{1/2}$. Each subsequent $\cos\theta$ is calculated according to

$$\cos\theta = \cos\theta^0 \cos\chi + \frac{X}{\chi}\sin\theta^0 \sin\chi, \tag{11}$$

where

$$X = r_{g1} + \frac{D\Delta t}{kT}(\mu E + pE^2\cos\theta^0)\sin\theta^0$$

and

$$\chi = (X^2 + r_{g2}^2)^{1/2}.$$

Again LCS is rotated in PCS as in the general procedure. For each step the mean value of $\cos^2\theta$ for all particles is evaluated and used for the calculation of the reduced electric dichroism according to the equation[2]

$$\Delta\epsilon/\bar{\epsilon} = (\Delta\epsilon/\bar{\epsilon})_\infty \frac{3\langle\cos^2\theta\rangle - 1}{2}. \tag{12}$$

E. Models and technical details of simulations

84 *bp DNA*: The DNA molecule with 84 base pairs is modeled by a linear, rigid string of 23 overlapping beads with a radius of 12 Å. The centers of subsequent beads are displaced by $r = 12$ Å and thus the maximal extension of the model is 288 Å. The rotational diffusion coefficient of the model, calculated according to procedures described by

Garcia de la Torre and Bloomfield[29] with the volume correction[30] introduced by Antosiewicz and Porschke,[31] is $0.340\times10^{6}\ s^{-1}$, corresponding to a dichroism decay time of 490 ns at 20 °C. This value is larger than the experimental one[32] (467 ns in 1 mM NaCl, 1 mM Na-cacodylate, 100 μM $MgCl_2$, *p*H 7.0); the difference, which is not important in the present context, is mainly due to the internal flexibility of the double helix. The extinction coefficients tensor is diagonal with $\epsilon_{xx,PCS}=\epsilon_{yy,PCS}=9100$ and $\epsilon_{zz,PCS}=1300$ ($M^{-1}\,cm^{-1}$) corresponding to a limiting reduced dichroism -1.2, in agreement with experimentally determined values. In the buffer mentioned above, the 84 bp DNA is characterized by a polarizability 5.80×10^{-33} C $m^2\,V^{-1}$, where the polarizability tensor P is assumed to be diagonal with the components $P_{xx}=P_{yy}=0$, and P_{zz} equal to the value just given. However, during calculations smaller values of the polarizability appeared to be more appropriate for the generation of characteristic effects in the "standard" range of electric field strengths and thus the following values were used: 1.67×10^{-33} C $m^2\,V^{-1}$ for the polarizability and 1.67×10^{-27} C m for the permanent dipole moment. These parameters are used for the whole system, i.e., the DNA double helix including counterions. The time steps for the simulation of 84 bp DNA varied from 5 ns at 10 kV/cm to 0.2 ns at 200 kV/cm.

Model corresponding to α-chymotrypsin: The dipole moment used for the 84 bp DNA model corresponds to the dipole moment measured for α-chymotrypsin.[33] For a direct comparison with experimental data we have also performed simulations for an object with a diffusion coefficient corresponding to that of α-chymotrypsin. The rotational diffusion coefficient $0.575\times10^{7}\ s^{-1}$ was calculated from the experimental dichroism decay time constant [(29 ns (Ref. 33)] according to the equation $\tau=1/6D$; the dipole moment was 1.67×10^{-27} C m ($\equiv$500 D). The time steps used during simulations for the chymotrypsin-like molecule varied from 2 ns at 10 kV/cm to 0.2 ns at 100 kV/cm.

tRNA: For the simulations of $tRNA^{Phe}$ we recalculated the previous results[34] using our volume correction,[31] which is now applied for all of our simulations (previously we used the corrections according to Garcia de la Torre and Rhodes[30]). We start from the crystal structure data for $tRNA^{Phe}$ (yeast) published by Ladner *et al.*[35] and substitute each nucleotide by one bead as described previously.[34] We used a mean bead radius 8.2 Å. The "accessible volume" of the model is 3.6×10^{4} Å^3. The generalized diffusion tensor of the model is calculated and subsequently transformed to its center of diffusion. We have rotated the model such that the beads corresponding to nucleotides 34 and 36, i.e., first and third of the anticodon, are parallel to the *z* axis. The resulting coordinate system is used to calculate the extinction coefficient tensor and dipole moment resulting from partial charges on individual phosphate atoms as described previously.[34] We used an effective charge on each phosphate residue corresponding to 15% of the elementary charge; this charge was assigned to the center of each bead. The approximations used for the calculation of the dipole do not seriously limit the validity of our simulation, because we are mainly interested in the influence of the translational–rotational coupling on the alignment of the particle under rectangular electric field pulses. For a detailed comparison we present some numerical values of our model: the dipole moment is 7.5×10^{-28} C m (relative to the center of diffusion), the rotational relaxation time at 20 °C is 30.3 ns (apparent value from fitting by single exponential[34]) and limiting reduced dichroism is -0.38. The data are somewhat different from those resulting from our previous investigation due to the new volume correction. However, these differences are not essential in the context of the present investigation. The charge q introduced into equation (8) is the total effective charge of the molecule corresponding to $76\times0.15\times e$, where e is the elementary charge.

The time steps used for the simulation of tRNA varied from 4 ns at 20 kV/cm to 0.15 ns at 400 kV/cm.

III. RESULTS AND DISCUSSION

Our Brownian dynamics simulations provide data, which are analogous to experimental data obtained from standard electrooptical measurements. An example for a dichroism rise curve simulated for the chymotrypsin-like model at 20 kV/cm is shown in Fig. 1. The curve represents an average signal from 1.2×10^{6} particles calculated with a time step of 1.1 ns. In complete analogy with standard experimental data we may extract information on the time constant(s) and on the stationary level of the dichroism. Both parameters have been characterized over a wide range of the electric field strength. As should be expected, the stationary dichroism found for the chymotrypsin-like molecule at different field strengths is fitted at a high accuracy by the orientation function for permanent dipoles (cf. Fig. 2) with a dipole moment and a limiting dichroism corresponding exactly to that introduced in the simulations. Equivalent results have been obtained from all simulations, which confirm the validity of our simulation procedure.

The validity of our approach has also been tested by analysis of the dichroism decay curves. The rotational relax-

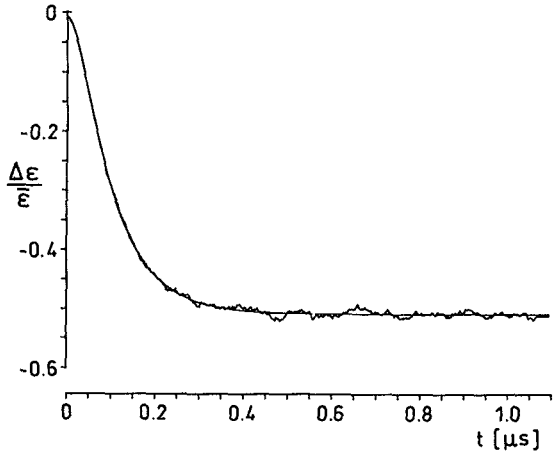

FIG. 1. Dichroism rise curve obtained from a Brownian dynamics simulation for the chymotrypsin-like model at 20 °C. Electric field strength 20 kV/cm; number of the particles used in the simulation is 1.2×10^{6}; time step 1.1 ns. The line without noise represents a least-squares fit by a sum of two exponentials with an initial zero slope; $\tau_1=27.3$ ns, $\tau_2=81.4$ ns.

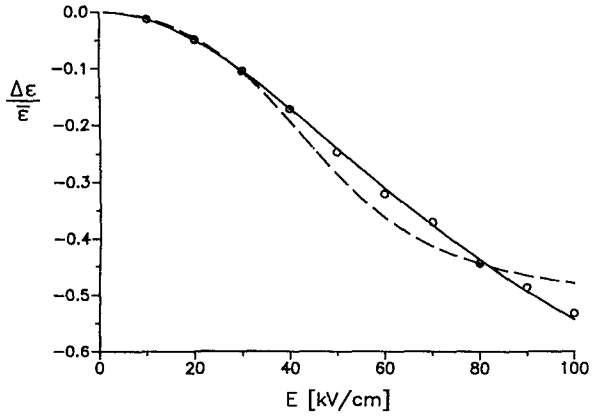

FIG. 2. Reduced linear dichroism $\Delta\epsilon/\bar{\epsilon}$ of the chymotrypsin-like molecule, with an implemented permanent dipole moment of 1.67×10^{-27} C m, as a function of the field strength E. The continuous line represents a fit according to a permanent dipole moment with $\mu = 1.61\times10^{-27}$ C m and $(\Delta\epsilon/\bar{\epsilon})_\infty = -1.25$; the dashed line represents a least-squares fit according to an induced dipole moment.

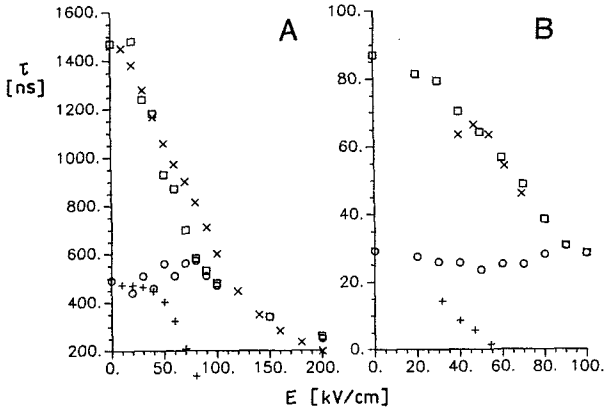

FIG. 3. Relaxation time constants τ_1 (○) and τ_2 (□) obtained for rise curves of the electric dichroism at different electric field strengths E: (A) 84 bp DNA model with $\mu = 1.67\times10^{-27}$ C m and $D_r = 0.340\times10^6$ s^{-1}; (B) for the chymotrypsin-like molecule with $\mu = 1.67\times10^{-27}$ C m and $D_r = 0.575\times10^7$ s^{-1}. For comparison, corresponding time constants τ_1 (+) and τ_2 (×) are given in panel A from fits to rise curves generated according to Matsumoto *et al.*[11] with the parameters of the 84 bp model and in panel B from dichroism rise curves measured for α-chymotrypsin Ref. 33 [20 °C; for both models $(\Delta\epsilon/\bar{\epsilon})_\infty = -1.2$; standard deviation of the simulated time constants are for model A 50 ns at 10–20 kV/cm to 20 ns at 100 kV/cm and for model B from 5 ns at 20 kV/cm to 2 ns at 100 kV/cm].

ation times derived from these curves correspond to the implemented rotational diffusion coefficient ($\tau = 1/6D_r$) within the limits of accuracy and are independent of the field strength used for the alignment. These data will not be discussed in further detail, because we are mainly interested in the electrooptical transients found in the presence of electric fields.

As shown in Fig. 1 for the example of the chymotrypsin-like model, electrooptical rise curves for molecules with an implemented permanent dipole moment require two exponentials for a satisfactory fit. The two exponentials, with amplitudes in opposite direction, superimpose to resulting curves with zero slope at time zero. Electrooptical rise curves of this type were predicted by Benoit[6] for molecules with permanent dipole moments in the limit of very low electric field strengths. According to Benoit one of the time constants corresponds to the electrooptical decay time constant τ_d (≡ rotational relaxation time constant) and the other one to $3\times\tau_d$. Benoit's treatment, valid for very low electric field strengths E, was subsequently extended for arbitrary E values,[7-11] but the extensions remained restricted to particles with cylindrical symmetry. The Brownian dynamics approach is not limited with respect to particle symmetry or the magnitude of the electric field strength and, thus, any dependence can be followed without restriction. Electrooptical rise curves have been simulated for our two models with cylindrical symmetry up to very high electric field strengths; the results obtained by exponential fitting are shown in Fig. 3. In both cases we find a clear decrease of the larger relaxation time constant τ_2 with increasing electric field strength E, whereas the smaller time constant τ_1 is found to be almost independent of E. At high field strengths the values for the time constants τ_1 and τ_2 are very close to each other. In the limit of low field strengths both time constants approach the values expected according to the analytical treatment of Benoit. The "noise" of the time constants shown in Fig. 3 is *due to* the limited number of particles included in the simulation. A decrease of this noise would be possible simply by increasing the number of particles, but would cost much computer time.

For comparison we have included in Fig. 3 some relaxation time constants evaluated from rise curves generated according to Eq. (36) of Matsumoto *et al.*[11] Up to 30 kV/cm these time constants are in very satisfactory agreement with the results obtained from Brownian dynamics. Deviations observed at higher field strengths result from the fact that the equation of Matsumoto *et al.* is limited to terms up to E^6 (sixth-order perturbation) and is valid for relatively low fields.

For the case of the chymotrypsin-like model we show in Fig. 3 also some experimental data obtained from measurements of the electric dichroism.[33] The experimental time constants τ_2 are in satisfactory agreement with the Brownian dynamics result. However, a clear deviation is found for the time constants τ_1: the experimental τ_1 values decrease very strongly with increasing electric field strengths E, whereas the corresponding simulated values are almost independent of E. These deviations are observed at rather high E values and thus it may be suspected that the experimental data are affected by some "hidden" contribution from an induced dipole moment, which shows up at high E due to the E^2 dependence. This result indicates that the time constants measured as a function of the electric field strength may be more sensitive than measurements of the stationary dichroism as a function of the electric field strength.

We have also simulated electrooptical rise curves for induced dipoles. As should be expected these curves can be fitted by single exponentials at high accuracy. The time constants resulting from these fits (cf. Fig. 4) show two limit ranges with respect to their dependence on the electric field strength. At very low E values the time constant is equiva-

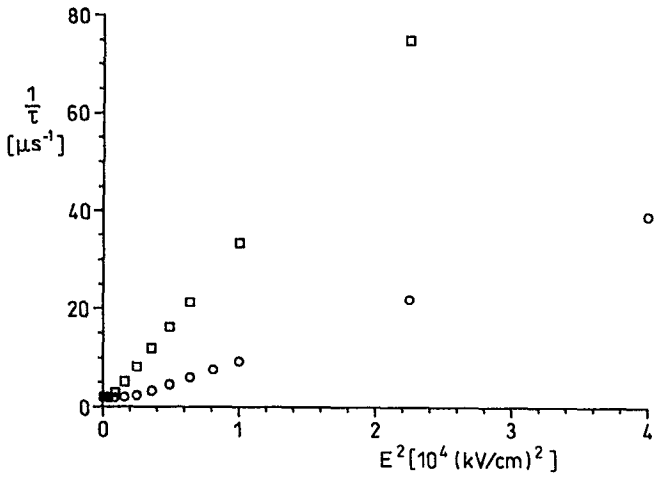

FIG. 4. Reciprocal relaxation time constants from dichroism rise-curves simulated for the 84 bp DNA model as a function of the square of the electric field strength E^2 with two different values of the implemented polarizability: 1.67 and 5.80×10^{-33} C m^2 V^{-1} (○ and □, respectively).

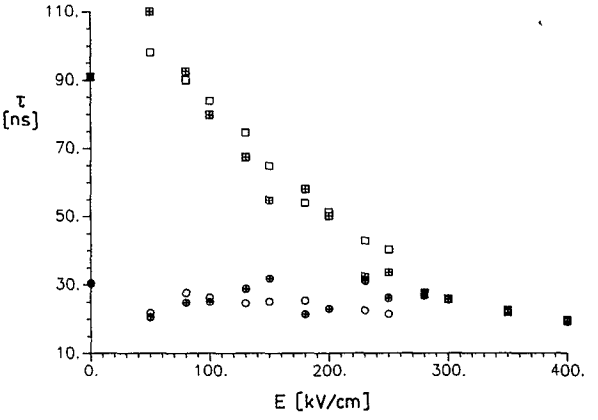

FIG. 6. Relaxation time constants τ_1 (○) and τ_2 (□) from dichroism rise-curves simulated for tRNA as a function of the electric field strength E. The symbols marked with " + " show the data calculated with hydrodynamic coupling, the empty ones without hydrodynamic coupling. The filled symbols at $E=0$ represent the time constants expected according to Benoit (Ref. 6). The standard deviations σ at 50 kV/cm are $\pm$ 8 ns for τ_1 and $\pm$ 16 ns for τ_2; the σ values decrease gradually with increasing E and are $\pm$ 3 ns at 300 kV/cm. The results at 50 kV/cm are averaged from simulations for 2.4×10^6 particles; the number of particles was decreased gradually for larger fields and is 6×10^4 at 400 kV/cm.

lent to that associated with "free" rotational diffusion, whereas the electric torque is dominant at high E values. For the latter range, where free diffusion is negligible, we find a linear dependence of $1/\tau$ on E^2. According to Schwarz,[7] this dependence is expected for induced dipoles with cylindrical symmetry in the limit of very high electric fields and should be consistent with

$$1/\tau = \frac{2pD_r}{kTx_0}E^2, \tag{13}$$

where p is the polarizability along the main axis, D_r the rotational diffusion coefficient about the main axis and x_0 a factor, which is approximately 3.35 according to Schwarz.

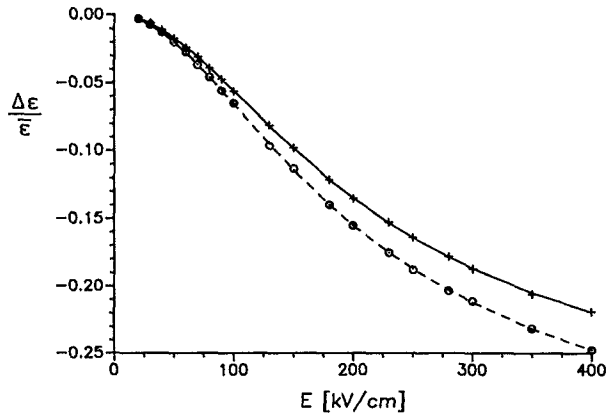

FIG. 5. Stationary reduced dichroism $\Delta\epsilon/\bar{\epsilon}$ for tRNA at different electric field strengths E simulated without (○, dashed line) and with (+ , continuous line) hydrodynamic coupling. The lines represent least-squares fits according to a permanent dipole orientation function $\mu = 7.48$ and 7.19×10^{-28} C m and $(\Delta\epsilon/\bar{\epsilon})_\infty = -0.381$ and -0.345 without and with hydrodynamic coupling, respectively; corresponding fits for the range of electric field strengths up to 100 kV/cm (used for dichroism experiments) provide $\mu = 7.29$ and 7.27×10^{-28} C m and $(\Delta\epsilon/\bar{\epsilon}_\infty) = -0.397$ and -0.341 without and with hydrodynamic coupling, respectively.

From the slopes in the linear part of the data given in Fig. 4 and from the polarizabilities 1.67 and 5.80×10^{-33} C m^2 V^{-1} used in the simulations, we arrive at factors $x_0 = 2.86$ and 2.93, respectively. Because the difference between our simulated x values is within the limits of accuracy and because Schwarz has given his x_0 value only approximately, we propose to use $x_0 = 2.90$ for future evaluations of experimental data according to Eq. (13).

Finally, we have simulated electrooptical transients for tRNA, a molecule without symmetry. In this case the components of the generalized diffusion tensor describing the coupling of translational and rotational diffusion are not zero and thus some influence of the electrophoretic motion on the electrooptical data may be expected. For comparison electrooptical data were simulated with and without translational–rotational coupling. As shown in Fig. 5, the diffusional coupling has a relatively small, but noticeable effect on the stationary dichroism. Least-squares fitting by the permanent dipole orientation function shows that the hydrodynamic interactions lead to a reduction of the apparent dipole moment by $\approx$5% and of the limit reduced dichroism by $\approx$10%. In the case of the electrooptical rise time constants (cf. Fig. 6), any influence of the hydrodynamic coupling is hardly detectable. Thus, we may conclude that the effect of translational–rotational coupling is rather small, at least for the case of tRNA^{Phe} (yeast). Apparently diffusional coupling effects may have a clearly detectable influence on electrooptical data only for very special conditions.[14]

Our present simulations clearly demonstrate the advantages of the Brownian dynamics procedures. The "computer experiments" help to characterize contributions to experimental results, which are very hard to identify otherwise. Usually analytical results are available only for very restricted ranges of conditions, whereas simulations can be extended without restrictions. Owing to the rapid development

of computer technology, restrictions due to limited computer time are not really serious anymore and are expected to be even less serious in the future. In our present investigation we have been able to obtain results on electrooptical parameters without restrictions on the electric field strength and on particle symmetry. We have also been able to analyze the influence of translational–rotational coupling. The particles used in our simulations were rigid. In future simulations it should be possible to include effects due to internal flexibility and counterion fluctuations. Thus, the new approach to the interpretation of complex electrooptical data, which is now accessible by Brownian dynamics procedures, is expected to provide additional important information in the future.

ACKNOWLEDGEMENTS

All calculations were performed using facilities of the Gesellschaft für wissenschaftliche Datenverarbeitung mbH, Göttingen. We thank Gerhard Nolte for vectorization of our programs. J. A. was supported by Max-Planck-Gesellschaft and by Ministry of National Education (Poland) within the Project CPBP 01.06.

[1]C. T. O'Konski, K. Yoshioka, and W. H. Orttung, J. Phys. Chem. **63**, 1558 (1959).
[2]E. Fredericq and C. Houssier, *Electric Dichroism and Electric Birefringence* (Clarendon, Oxford, 1973).
[3]*Molecular Electrooptics*, edited by C. T. O'Konsky (Marcel Dekker, New York, part 1, 1976, part 2, 1978).
[4]*Molecular Electrooptics*, edited by S. Krause (Plenum, New York, 1980).
[5]E. Charney, Q. Rev. Biophys. **21**, 1 (1988).
[6]H. Benoit, Ann. Phys. **6**, 561 (1951).
[7]G. Schwarz, Z. Phys. **145**, 563 (1956).
[8]I. Tinoco, Jr. and K. Yamaoka, J. Phys. Chem. **63**, 423 (1959).
[9]K. Nishinari and K. Yoshioka, Koll.-Z. Z. Polymere **235**, 1189 (1968).
[10]G. de Groot, W. Boontje, J. Greve, and H. J. Boersma, Biopolymers **16**, 1377 (1977).
[11]M. Matsumoto, H. Watanabe, and K. Yoshioka, J. Phys. Chem. **74**, 2182 (1970).
[12]W. A. Wegener, R. M. Dowben, and V. J. Koester, J. Chem. Phys. **70**, 622 (1979).
[13]D. B. Roitman and B. H. Zimm, J. Chem. Phys. **81**, 6348 (1984).
[14]W. A. Wegener, J. Chem. Phys. **84**, 5989 (1986).
[15]A. Szabo, M. Haleem, and D. Eden, J. Chem. Phys. **85**, 7472 (1986).
[16]S. Nath, J. S. Bowers, and R. K. Prud'homme, J. Chem. Phys. **89**, 5943 (1988).
[17]W. E. Sonnen, G. E. Wesenberg, and W. E. Vaughan, Biophys. Chem. **32**, 283 (1988).
[18]D. L. Ermak and J. A. McCammon, J. Chem. Phys. **69**, 1352 (1978).
[19]E. Dickinson, Chem. Soc. Rev. **14**, 421 (1985).
[20]S. C. Harvey and H. C. Heung, Proc. Natl. Acad. Sci. USA **69**, 3670 (1972).
[21]R. J. Lewis, S. A. Allison, D. Eden, and R. Pecora, J. Chem. Phys. **89**, 2490 (1988).
[22]S. Allison, R. Austin, and M. Hogan, J. Chem. Phys. **90**, 3843 (1989).
[23]H. Brenner, J. Colloid. Interface Sci. **23**, 407 (1967).
[24]H. Goldstein, *Classical Mechanics* (Addison-Wesley, Cambridge, MA, 1953).
[25]K. V. Mardia, *Statistics of Directional Data* (Academic, London, 1972).
[26]D. Porschke and M. Jung, J. Biomol. Struct. & Dyn. **2**, 1173 (1985).
[27]S. Diekmann, W. Hillen, M. Jung, R. D. Wells, and D. Porschke, Biophys. Chem. **15**, 157 (1982).
[28]G. Bialkowski, *Mechanika klasyczna* (Polish Science, Warszawa, 1975).
[29]J. Garcia de la Torre and V. A. Bloomfield, Q. Rev. Biophys. **14**, 81 (1981).
[30]J. Garcia de la Torre and V. J. Rodes, J. Chem. Phys. **79**, 2454 (1983).
[31]J. Antosiewicz and D. Porschke, J. Phys. Chem. **93**, 5301 (1989).
[32]D. Porschke, Biopolymers **28**, 1383 (1989).
[33]J. Antosiewicz and D. Porschke, Biochemistry **28**, 10 072 (1989).
[34]D. Porschke and J. Antosiewicz, Biophys. J. **58**, 403 (1990).
[35]J. E. Ladner, A. Jack, J. D. Robertus, R. S. Brown, D. Rhodes, B. F. C. Clark, and A. Klug, Nucleic Acids Res. **2**, 1629 (1975).